

PII:S0967-0661(96)00056-1

## AN ADAPTIVE SCHEME WITH AN OPTIMALLY TUNED PID CONTROLLER FOR A LARGE MSF DESALINATION PLANT

A. Woldai\*, D.M.K. Al-Gobaisi\*, R.W. Dunn\*\*, A. Kurdali\* and G.P. Rao\*\*\*,1

\*Water and Electricity Department, Government of Abu Dhabi, Abu Dhabi, UAE

\*\*University of Bath, Bath, UK

\*\*\*IFFWSAT. Abu Dhabi. UAE

(Received July 1995; in final form March 1996)

Abstract: This paper reports on the experience in the course of development of an adaptive control strategy for an 18-stage multistage flash (MSF) desalination plant presently operating in the Arabian Gulf region. The parameter-scheduling strategy maintains optimality of PID controllers over the operating region and is derived by simulation using a detailed phenomenological dynamic model. An optimal method of reducing the model into first-order-dead-time (FODT) form and a non-parametric model-based simulation facility are presented. Based on a relative gain array analysis, an appropriate control structure has been established. A number of integral performance criteria have been used, without resorting to the use of a reduced model, directly with the non-parametric simulation facility for optimal controller tuning. The controller parameters are given as a vector function of the top brine temperature (TBT) and the brine recycle flow rate, which are key variables for the TBT control.

Keywords: Relative gain analysis, PID control, nonparametric models, simulation, adaptive control, parameter scheduling, nonlinear control, MSF desalination.

### 1. PROCESS DESCRIPTION, LINEARISED DYNAMIC MODEL AND ITS FEATURES

1.1 Multistage Flash Desalination Process (MSFDP).

The multistage flash desalination process (MSFDP) is an evaporation-condensation process which is a major means of desalting seawater at present. It is almost similar to the process (sans flashing) of evaporation, cloud formation and precipitation that occurs in nature, giving rain. In view of this similarity, it is a process in close harmony with nature. While being instrumental in serving one of the basic needs of humanity, it is considered as one which causes little environmental pollution or ecological imbalance.

The MSF process basically consists of evaporation and condensation of water successively in a series of flash stages. These stages are maintained under progressively reduced pressure. The brine entering a particular stage is superheated with respect to the conditions inside that stage, as a result of which flashing occurs. The vapour generated is then condensed on the outside surface of a tube bundle provided in the upper portion of the stage, and the distillate falls into the product trough placed below the tube bundle. The heat released due to condensation is recovered by the incoming brine flowing through the tubes as a coolant. Thus, the multistage process shown in Fig. 1 consists of three streams, namely, the first of flashing brine flowing from stage 1 to stage N, secondly of cooling brine flowing inside the tubes countercurrently and the last of distillate product flowing in the same direction as that of the flashing brine.

The MSF evaporator comprises three main sections viz., the heat recovery sections, heat rejection

<sup>&</sup>lt;sup>1</sup> on leave from Indian Institute of Technology, Kharagpur, India

sections and a brine heater (Fig. 1). In the recovery stages 1 to NR, heat is recovered from the condensation of vapour by the recycle stream (i.e. cooling brine) flowing countercurrently inside the tubes from stage to stage. The recycled brine coming out from stage 1 is further heated to the maximum temperature in the process (known as "top brine temperature" or TBT) in the brine heater by low pressure steam, before it enters the first stage for flashing. Thus, the brine heater is the primary source of energy in the whole process. In the rejection stages, which are usually three in number, the fresh seawater flows as the coolant on the tube side, and part of the heat recovered in these stages is ejected to the sea. The remaining seawater after deaeration and the necessary chemical treatment enters as "makeup" into the last stage, N.

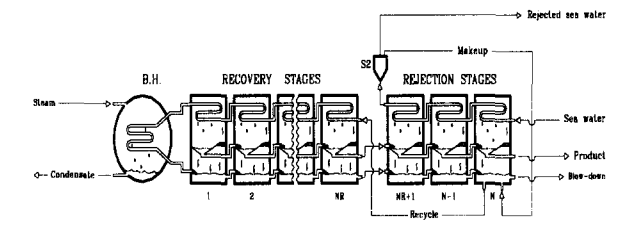


Fig. 1. Schematic flow diagram of MSF process plant.

#### Each flash stage includes:

- flash chamber in which the flashing occurs,
- tube bundle on which the condensation takes place,
- tray to receive the distillate, and
- the vapour space in between.

Figure 2 shows a cross-section of the chamber of a flash evaporator. Between the flash chamber and the vapour space are placed the demisters to remove entrained droplets from the vapour. Brine flows from one flash chamber to the next through a weir box or orifice which regulates the brine level in each stage in order to prevent blowthrough between the stages as well as pressure equalization. The last stage level is controlled by manipulating the blow-down flow, which is the ultimate discharge of concentrated brine to the sea.

A few stages are directly connected to the vacuum line for removing noncondensable gases and air leaks, while the others are cascaded for the same purpose.

The distillate similarly flows from stage to stage in the distillate trough and leaves from the final stage as the product, where its level in the trough is controlled.

The MSF plant works as part of a dual-purpose plant, utilizing low-pressure steam exhaust from the turbine as the heat source. Its efficiency mainly depends upon

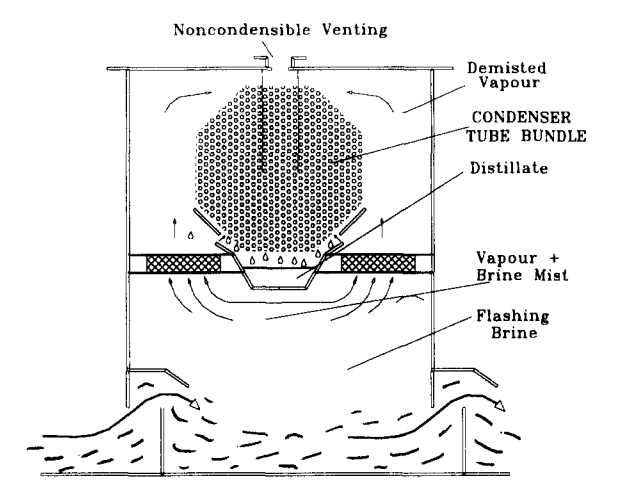


Fig. 2. Cross section of the chamber of a flash evaporator.

the "flash range", which is the difference between the TBT and the discharge temperature. The efficiency is measured in terms of a "Performance Ratio" (PR), which is approximately equal to Kg of product per Kg of steam condensed in the brine heater.

#### 1.2 MSF desalination plant control systems.

Several closed-loop control systems are typical of a modern MSFDP (Fig. 3). The controlled systems are as follows (Al-Gobaisi et al., 1991, 1993; Al-Gobaisi, 1995):

#### Brine heater section

- 1. Top brine temperature
- 2. Temperature of low-pressure steam
- 3. Pressure of LP steam
- 4. Level of brine heater condensate
- 5. Conductivity of brine heater condensate.

Condenser section (recirculation and make up flow)

- 6. Flowrate of brine recirculation
- 7. Make-up flowrate
- 8. pH-value of recirculating brine feed
- 9. Antiscale dosing (or antiscale/make-up ratio)
- 10. Sodium sulphite injection into brine recirculation stream.

#### Evaporator section

- 11. Brine level in the last stage
- 12. Distillate level in the last stage
- 13. Flowrate of flow down
- 14. Conductivity of distillate
- 15. Chloride injection into distillate
- pH-value of output distillate (lime/caustic soda injection into distillate).

#### Cooling section

- 17. Flow of seawater to heat reject section
- 18. Inlet temperature of cooling water
- 19. Minimum flow of seawater.

#### Ejector and venting section

- 20. Level of condensate in ejector
- 21. Conductivity of ejector condensate
- 22. Vacuum pressure of the last stage of the evaporator.

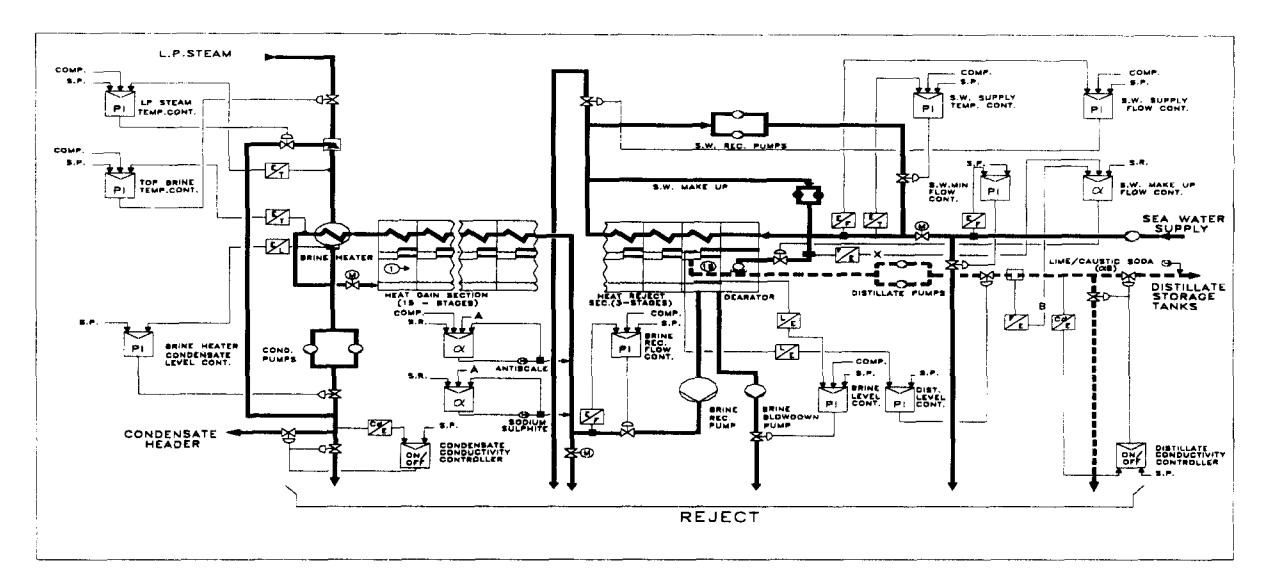


Fig. 3. MSF desalination process.

#### 1.3 Modelling and simulation

Modelling refers to formulating a set of equations that mathematically describe any industrial process under consideration (Barba et al., 1973). In the simulation phase, the formulated model is solved using a suitable solution procedure, as well as entering the values of input process parameters. Modelling and simulation in the process industry may have different goals, such as improving and optimizing designs, developing better insight into the working of the process, and ultimately leading to the optimal operation and control of the process.

The following are the salient features of modelling and simulation carried out on an 18-stage MSFDP (Husain, et al., 1993). The brine heater is divided into 10 sections and each flash stage is considered as one lump. The various subsystems are described by appropriate mass and energy balance equations. The interstage orifices are described by the related hydraulic models. The control valves, and other subsystems and components, have been modelled similarly. The design parameters of these, as in the actual plant given by plant designers, are inserted in a flowsheet simulator. Table 1 shows the result of steady-state simulation with the given operating conditions. The result shows the temperatures of the brine, distillate and cooling tubes in the 18 flash stages. Table 2 compares summer temperature profiles in the flash chambers, by simulation, with those obtained by actual measurement on the plant. The good agreement between the temperature profiles of the model and the actual plant should be viewed only as a partial success in model validation.

#### 1.4 Dynamic simulation and model verification

The model of the MSF plant is simulated under the following conditions of dynamic run with all loops closed for comparison with the plant test response.

The model response is shown in Fig. 4, together with the actual plant response to a TBT setpoint change as indicated.

Table 1 Steady-state performance of the MSF plant

Operating conditions:		
Steam Flow	165.733	[t/hr]
Reject Flow	6297.182	[t/hr]
Recycle Flow	14419.995	[t/hr]
Make Up Flow	6142.800	[t/hr]
Blowdown Flow	4919.913	[t/hr]
Top Brine Temperature	95.000	[C]
Product Flow	1219.131	[t/hr]
Seawater Flow	12439.982	[t/hr]
Performance Ratio	7.312	[kg/540 kcal]

Sta-	TF_IN	D_OUT	TD_OUT	B_OUT	TB_OUT
ges					
1	85.102	1.323	90.640	238.977	91.712
2	81.897	2.628	87.432	237.666	88.502
3	78.702	3.915	84.242	236.377	85.313
4	75.524	5.183	81.056	235.107	82.137
5	72.360	6.432	77.894	233.856	78.979
6	69.214	7.662	74.744	232.625	75.839
7	66.087	8.873	71.615	231.412	72.716
8	62.981	10.063	68.502	230.220	69.616
9	59.900	11.234	65.412	229.048	66.541
. 10	56.845	12.383	62.344	227.897	63.491
11	53.822	13.509	59.296	226.769	60.475
12	50.837	14.612	56.279	225.666	57.497
13	47.893	15.689	53296	224.587	54.560
14	44.994	16.740	50.348	223.535	51.670
15	42.134	17.769	47.452	222.505	48.820
16	40.651	18.554	45.282	221.719	46.625
17	38.039	19.363	42.908	220.908	44.348
18	35.000	20.319	40.751	81.999	42.134

(TF\_IN, TD\_OUT and TB\_OUT represent the temperature profile in the cooling brine, distillate and brine chamber respectively. D\_OUT is the distillate output and B\_OUT the flow in a brine chamber).

<u>Table 2 Comparison of Summer Temperature</u> <u>Profiles Results obtained from Simulated (Sim) and</u> <u>Observed (Obs) in Steady-State</u>

	Simulated	Observed
Make up flow	5520	5516 [t/hr]
Blowdown flow	4383	4376 [t/hr]
Product flow	1133	1140 [t/hr]
Reject flow	8988	8983 [t/hr]
Top Brine Temperature	90°C	90° [C]
Performance Ratio	7.20	7.02[kg/540 cal]

T21 1			D:	4111	Q 1:	70.1	
Flash		Brine		Distillate		Cooling Tube	
Stage	(	(°C)		(°C)		(°C)	
No.	Sim	Obs	Sim	Obs	Sim	Obs	
1	86.95	87.03	85.88	85.93	80.71	80.70	
2	83.97	84.11	82.90	83.03	77.73	77.79	
3	81.00	81.20	79.93	80.12	74.76	74.89	
4	78.06	78.23	76.97	77.15	71.81	71.93	
5	75.13	75.28	74.04	74.18	68.88	68.98	
6	72.22	72.35	71.12	71.24	65.96	66.06	
7	69.32	69.44	68.21	68.32	63.06	63.16	
8	66.45	66.56	65.33	65.41	60.18	60.28	
9	63.60	63.71	62.46	62.54	57.33	57.43	
10	60.78	60.89	59.62	59.67	54.50	54.62	
11	57.98	58.09	56.79	56.87	51.70	51.82	
12	55.23	55.33	53.99	54.06	48.94	49.07	
13	52.51	52.62	51.23	51.29	46.21	46.35	
14	49.83	49.95	48.50	48.56	43.53	43.69	
15	47.20	47.33	45.81	45.88	40.88	41.07	
16	45.03	45.16	43.61	43.68	39.29 <sup>f</sup>	39.24	
17	42.91	43.02	41.44	41.53	37.21	37.13	
18	40.88	40.88	39.51	39.45	35.00	35.00	

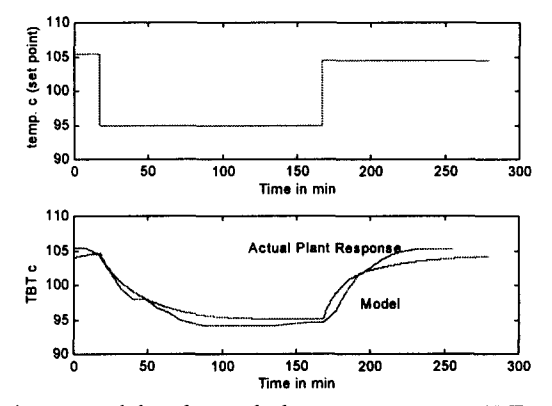


Fig. 4. Model and actual plant response to a TBT setpoint change.

The model is acceptable in view of its satisfactory agreement in dynamic behaviour with the actual plant, for further considerations such as analysis and control-system design.

#### 1.5 Model linearization

A process is generally described by a set of nonlinear ordinary differential and algebraic equations of the form:

$$\dot{x}(t) = f\left[x(t), u(t)\right] \tag{1}$$

$$y(t) = g\left[x(t), u(t)\right] \tag{2}$$

where

$$x(t) = [x_1(t) \quad x_2(t) \quad \dots \quad x_n(t)]^T$$
 (3)

$$y(t) = [y_1(t) \quad y_2(t) \quad \dots \quad y_m(t)]^T$$
 (4)

$$u(t) = \begin{bmatrix} u_1(t) & u_2(t) & \dots & u_r(t) \end{bmatrix}^T$$
 (5)

and f and g are n and m vector valued functions of the state x(t) and the inputs u(t). Equations (1) and (2) are known as the state and output equations respectively.

Consider a steady-state operating condition  $\bar{x}$ ,  $\bar{u}$  and let the process be perturbed by small signals  $x^*(t)$  and  $u^*(t)$  such that

$$x(t) = \overline{x} + x^{\bullet}(t)$$

$$u(t) = \overline{u} + u^{\bullet}(t).$$
(6)

Equation (1) is linearized to appear in the form

$$x^{\bullet}(t) = Ax^{\bullet}(t) + Bu^{\bullet}(t) \tag{7}$$

where

$$A = \begin{bmatrix} \frac{\partial f_1}{\partial x_1} & \cdots & \frac{\partial f_1}{\partial x_n} \\ \vdots & \vdots & \ddots \\ \frac{\partial f_n}{\partial x_1} & \cdots & \frac{\partial f_n}{\partial x_n} \end{bmatrix}_{\substack{x = \bar{x} \\ u = \bar{u}}}$$
 (8)

and

$$B = \begin{bmatrix} \frac{\partial f_1}{\partial u_1} & \dots & \frac{\partial f_1}{\partial u_r} \\ \vdots & \ddots & \ddots \\ \frac{\partial f_n}{\partial u_1} & \dots & \frac{\partial f_n}{\partial u_r} \end{bmatrix}_{\substack{x = \bar{x} \\ n = \bar{u}}}$$
(9)

Similarly, Equation (2) is linearized into the form

$$y^*(t) = Cx^*(t) + Du^*(t)$$
 (10)

where

$$C = \begin{bmatrix} \frac{\partial g_1}{\partial x_1} & \dots & \frac{\partial g_1}{\partial x_n} \\ \vdots & \vdots & \ddots \\ \frac{\partial g_m}{\partial x_1} & \dots & \frac{\partial g_m}{\partial x_n} \end{bmatrix}_{x=\bar{x}}$$
(11)

and

$$D = \begin{bmatrix} \frac{\partial g_1}{\partial u_1} & \cdots & \frac{\partial g_1}{\partial u_r} \\ \vdots & \vdots & \ddots \\ \frac{\partial g_m}{\partial u_1} & \cdots & \frac{\partial g_m}{\partial u_r} \end{bmatrix}_{\substack{r=\bar{x} \\ u=\bar{u}}}$$
(12)

For notational simplicity, Eqs (7) and (10) are written without the asterisk as

$$\dot{x} = Ax + Bu \tag{13}$$

$$y = Cx + Du. (14)$$

These are the linearized state-space equations about  $(\bar{x}, \bar{u})$ . Control-system design is based on these equations. The linear model and the related controller are valid in the close neighbourhood of the operating point  $\bar{x}, \bar{u}$ .

#### 1.6 Linearized model of an MSF plant

The model of the present MSF plant is set up in a SPEEDUP flow-sheet simulator. Operating conditions i.e. TBT - 95°C, and Recycle Flow of 14420 t/hr have been chosen and the model is linearized at this condition using a dynamic run and invoking the control design interface (CDI) of SPEEDUP with the following 6 inputs and 6 outputs:

Manipulated variables (inputs)

u<sub>1</sub> : Culvert controller output
 u<sub>2</sub> : Makeup controller output
 u<sub>3</sub> : Brine recycle controller output

 $u_4$ : Seawater recirculation controller output

 $u_5$ : Reject controller output  $u_6$ : Steam controller output Controlled variables (outputs)  $y_1$ : Top brine temperature

 $y_2$ : Culvert flow

 $y_3$ : F18.Flow (seawater flow to reject section)

 $y_4$ : F18.Recycle flow (brine recycle)

 $y_5$ : Seawater recirculation flow (temperature)

 $y_6$ : Makeup flow.

CDI generates the matrices A,B,C and D of the state space and computes the steady-state gain matrix G(0).

The resulting linearized model has 155 state variables (7 per stage, the rest from the brine heater and integrals of controller errors).

From the linear state-space description of a multiinput-multi-output (MIMO) process in Eqs (13) and (14), the transfer function matrix between the inputs (manipulated variables) and the outputs (controlled variables) is given as

$$G(s) = C(sI - A)^{-1} B + D.$$
 (15)

The steady-state gain matrix or the d.c. gain matrix for non-integrating processes can be computed at s=0 in the above as

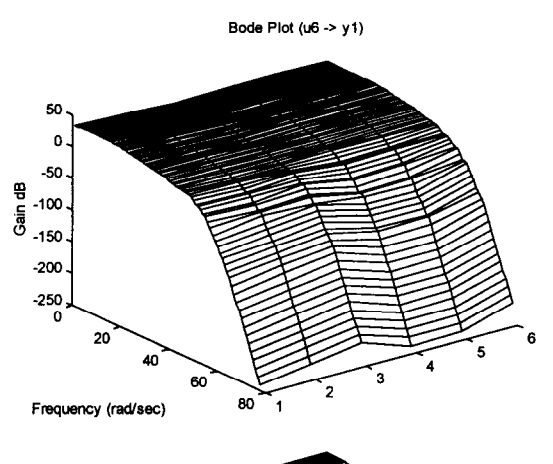
$$G(0) = -CA^{-1}B. {16}$$

In the case of integrating processes, i.e., those having poles at the origin of the s-plane (usually due to level-control systems),  $A^{-1}$  does not exist. Such situations will not be considered here.

The following is the d.c. gain matrix for a particular point of operation:

$$G_{95,14,42}(\sigma) = \begin{bmatrix} 0.000 & -2.188 & -82.032 & 0.106 & -2.801 & 54.002 \\ 61.70 & 176.243 & 0.0000 & 0.000 & 183.301 & 0.000 \\ 0.000 & 176.243 & 0.0000 & 96.70 & 183.301 & 0.000 \\ 0.000 & 0.0000 & 541.002 & 0.000 & 0.0000 & 0.000 \\ 0.000 & 0.0000 & 0.0000 & 3.497 & 0.0000 & 0.000 \\ 0.000 & 176.243 & 0.0000 & 0.000 & 0.0000 & 0.000 \end{bmatrix}$$

Figure 5 shows the Bode diagrams of  $G_{1.6}$ , in six different operating conditions, the most important of all elements in G(s). Cases 1-3 are TBT-95°C,  $100^{\circ}$ C,  $105^{\circ}$ C respectively, keeping the brine recycle flow fixed at 14420 t/hr, and Cases 4-6 correspond to a brine recycle flow of 11500 t/hr, 12500 t/hr, 13500 t/hr with TBT  $105^{\circ}$ C fixed respectively



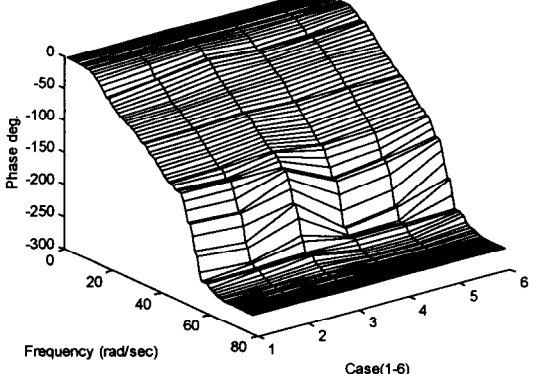


Fig. 5. G<sub>1.6</sub>(s) (unreduced) Bode diagrams.

## 2. CONTROL STRUCTURE, OPTIMAL PID TUNING BASED ON OPTIMAL FIRST ORDER PLUS DEAD TIME (FODT) APPROXIMATION

In this section the linearized model of the plant is considered for six inputs and six outputs. The transfer function matrix of the resulting model is subjected to interaction analysis by the well known relative gain array (RGA) method and an appropriate control structure has been established. The design of an optimal PID controller for one of the most important loops, namely the top brine temperature (TBT) loop is considered in detail. The model is then optimally approximated to the standard first-order plus dead time (FODT) form.

#### 2.1 Control structure.

The relative gain array  $\Lambda$  is a square matrix (for an equal number of manipulated and controller variables) whose columns refer to the manipulated variables and the rows to the controlled variables. That is

$$\Lambda = \begin{bmatrix}
\lambda_{11} & \lambda_{12} & \dots & \lambda_{1n} \\
\lambda_{21} & \lambda_{22} & \dots & \lambda_{2n} \\
\vdots & \vdots & \ddots & \vdots \\
\lambda_{n1} & \lambda_{n2} & \dots & \lambda_{nn}
\end{bmatrix}.$$

Some important properties of  $\Lambda$  are:

a) 
$$\sum_{j=1}^{n} \lambda_{ij} = 1, \text{ for all } i$$

#### b) $\lambda_{ij}$ is dimensionless.

From the d.c. gain matrix,  $\Lambda$  can be computed by using the relation

$$\Lambda = G(o) * [G(o)^{-1}]^T$$

where \* denotes element by element multiplication.

The manipulated and the controlled variables are so paired that the relative gains  $\lambda_{ij}$  are as close to unity as possible. That is, pair

(Controlled variable), with (manipulated variable),

if  $\lambda_{ii}$  is closest to 1. In all the six cases here

$$\Lambda = \begin{bmatrix} 0 & 0 & 0 & 0 & 0 & 1 \\ 1 & 0 & 0 & 0 & 0 & 0 \\ 0 & 0 & 0 & 0 & 1 & 0 \\ 0 & 0 & 1 & 0 & 0 & 0 \\ 0 & 0 & 0 & 1 & 0 & 0 \\ 0 & 1 & 0 & 0 & 0 & 0 \end{bmatrix}$$

clearly suggesting that the pairings are as follows  $(u_1 \rightarrow y_2)$ ,  $(u_2 \rightarrow y_6)$ ,  $(u_3 \rightarrow y_4)$ ,  $(u_4 \rightarrow y_5)$ ,  $(u_5 \rightarrow y_3)$  and  $(u_6 \rightarrow y_1)$ .

RGA analysis should also take into account the Niederlinski test for stability and is better done with  $G(j\omega)$  over a range of  $\omega$  around the Nyquist crossover point. Since the RGA analysis in all the cases here indicates a very clear pairing strategy, no further tests are needed.

#### 2.2 Model approximation for PID control design.

Reduced or approximated modelling of controlled processes in simple forms such as first-order or second-order with delay largely arises out of the widely prevailing PID control practice with possibilities for advanced features like optimization and adaptability. The multitude of model-reduction methods aimed at such simple forms, that are available in the literature varies in the degree of complexity and precision and ranges from crude rules of thumb (Smith and Corripio, 1985) and simple graphical schemes (Unbehauen and Rao, 1987) to optimization techniques (Seborg et al, 1989). Notwithstanding the effectiveness of the chosen optimization scheme, whether systematic or random-search-based, the need to account for fractional values (in terms of the sampling time interval) of delay in the desired model forms, necessitates an examination of the manner in which the objective function in the optimization method has to be computed. This seemingly trivial aspect is overlooked in most of the existing methods. An important contribution here lies in the proper handling of a possible fractional delay without rounding it into an integral multiple of the sampling time.

#### 2.3 Problem statement and method of approach.

The present problem of model reduction may be stated as follows:

"Given the step response  $h_o$  (t) of a large linear time invariant type zero asymptotically stable single-input/single-output system, find the transfer function  $G_r(p,s)$  of a reduced model  $G_r$  such that

$$J = \int_0^\infty \left[ h_o(t) - \ell^{-1} \left\{ s^{-1} G_r(\mathbf{p}, s) \right\} \right]^2 dt$$

is minimised subject to

$$h_o(\infty) = G_r(p,o)$$
  
 $p_i > 0$ 

for some specified i (parameters related to poles), and

$$p_n \geq 0$$

where **p** is an *n*-vector of parameters of  $G_r(\mathbf{p},s)$  and the *n*th element of **p** corresponds to a time delay."

In the computation of J, the common practice is to get the Z-transform  $G_r(\mathbf{q},z)$  of  $G_r(\mathbf{p},s)$  and then use the related difference equation to compute the step response of the reduced model as

$$h_r(kT) = Z^{-1}\{G_r(\mathbf{q},z)\}, \qquad k = 0,1,2,...,$$

where T is the sampling time. This procedure implies a rounding error when  $p_n/T$  is not an integer. In discretizing the continuous-time model, a zero order hold assumption is also required. Of course, this assumption is valid for the step input case. However, fractional delay may sometimes render the discrete time transfer function nonminimum phase. Furthermore, in general, when no information is available regarding input signals between the sampling instants, it is not possible to relate it to a continuous-time version.

In the present method, in view of the simplicity of the forms chosen for  $G_r(\mathbf{p},s)$  namely,

a) 
$$G_r(\mathbf{p},s) = \frac{K e^{-\theta s}}{(1+\tau s)}$$

or b) 
$$G_r(\mathbf{p}, s) = \frac{K(1+\tau_o s)}{(1+\tau_1 s)(1+\tau_2 s)}$$

 $h_r(t)$  may be analytically provided, avoiding the sampling process on the model. The continuous-time function corresponding to the delay-free portion of the chosen model can be shifted as desired and then sampled, to get the response of the continuous-time model with delay exactly at the required sampling instants for comparison with the given system response  $h_o(t)$ .

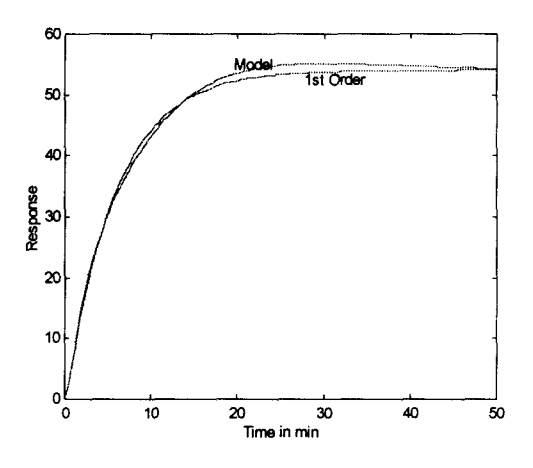
Next, minimization of J can be performed with the help of any standard routine. If an unconstrained minimization routine is available, the constraints can be applied externally. General routines for the time response of linear systems with a rigid vector of time instants should be avoided, because it will imply the same problem with fractional delays as mentioned above.

The matrices A, B, C, and D with the usual notation are obtained by linearization. The steady-state or dc gain matrix is easily computed as  $G(0) = -C A^{-1} B$  when the matrix A is nonsingular, i.e., if the integrating loops of the level control are closed and not considered in the input-output description. The minimal-realisation algorithm could remove only two redundant states out of the total of 155. Standard system-theoretic methods of model reduction could not reduce this minimal model to a tractably simple lower-

order form, since the system states (153 in number) are uniformly scattered, making the elimination procedure unsuccessful even with heavy tolerances. However, the step response of the large model could easily be computed and stored for reference in the present reduction procedure in which MATLAB was employed.

#### 2.4 Application of the present method.

The matrices A, B, C and D are first used to compute the dc gain matrix G(o). The step response of the original plant model is obtained by using the routine STEP of MATLAB at an adequate number of points in time until the response settles in steady-state. Figure 9 shows the step response matrices under the chosen conditions of operation (TBT, 95°C Brine Recyc 14420 t/hr). This data is used as reference. The algorithm is initiated with a parameter vector in the reduced model. The step response of the reduced model for this parameter vector is computed and used in the computation of the objective function J. The MATLAB routine FMINS is employed with external constraints to minimize J. Both the first- and secondorder forms with delay are fitted, and the results are shown for  $G_{1,6}$  in Fig. 6. Even the first-order approximation is quite impressive, but the secondorder approximation is excellent, indeed being able to capture the overshoot in the original step response.



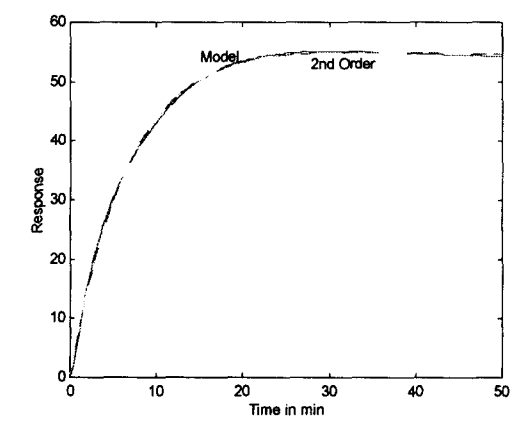


Fig. 6. Reduction of  $G_{95,14.42}(1,6)$  (with Recycle flow 14220 t/hr).

The corresponding frequency response functions are shown in Fig. 7 to give an idea of the approximation in the frequency domain as well. In the frequency band of interest, there is an excellent match both in magnitude and phase. The time scale is in units of minutes and the corresponding frequency is in radians per minute.

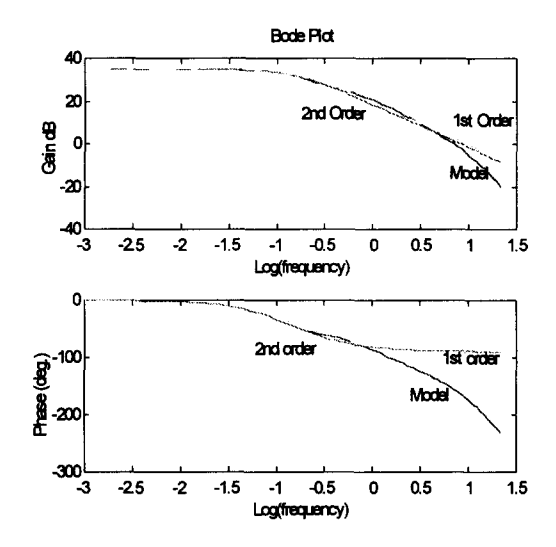


Fig. 7. G<sub>95,14,42</sub>(1,6). An approximation of first- and second-order in the frequency domain.

The transfer function matrices reduced to two levels of approximation, namely first and second, are given in Fig. 8 (a and b).

### 2.5 Optimal PID tuning with FODT approximated plant models

The RGA analysis has shown that simple SISO approach based control design is adequate for the plant as is evident from Section 1.1. Well established design methods (Zhuang and Atherton, 1993) can be applied to design controllers based on the FODT approximated model. The PID parameters can be read from precalculated tables if the parameters of the FODT model lie within the range of values for which the ready-made tables are available. There are situations in which the tables are not directly helpful, due to the model parameter values falling outside the limits. Moreover, the design is as good or as bad as the approximation itself. The repetition will avoid this obvious exercise and proceed further to avoid the approximation itself. Therefore, the aim here is to ensure optimal PID design without resorting to FODT approximation, which will be considered in Section 3.

# 3. PARAMETER SCHEDULING BASED ON OPTIMAL PID TUNING WITH AN UNREDUCED PLANT MODEL IN NONPARAMETRIC FORM

Optimal tuning of PID controllers based on integral performance criteria is by now well established, but the design relies on the standard first-order plus dead time (FODT) approximation of the plant model whose adequacy is not always guaranteed, and

	u <sub>1</sub>	u <sub>2</sub>	u <sub>3</sub>	u <sub>4</sub>	u <sub>5</sub> _	u <sub>6</sub>
$\mathbf{y}_1$	0	$\frac{-2.1884 e^{-1.4676s} (1 + 28.8135s)}{(1 + 17.522s)(1 + 17.522s)}$	$\frac{-82.032 e^{-0.0333s} (l + 24.878s)}{(l + 8.576s)(l + 8.460s)}$	0	$\frac{-2.8 \ e^{-6.5s}}{(1+10.98s)}$	$\frac{54 e^{-0.187s}}{(1+5.76s)}$
<b>y</b> <sub>2</sub>	61.7	176.2433	0	0	183.3005	0
<b>y</b> <sub>3</sub>	0	176.2433	0	$\frac{96.7}{(l+0.1s)}$	183.3005	0
y <sub>4</sub>	0	0	541.0021	0	0	0
<b>y</b> <sub>5</sub>	0	0	0	$\frac{3.496}{(l+0.1s)}$	0	0
<b>y</b> <sub>6</sub>	0	176.2433	0	0	0	0

Fig. 8 (a). Transfer function matrix with first-order plus delay approximation for G<sub>1.5</sub> & G<sub>1.6</sub>.

_	$u_1$	u <sub>2</sub>	$\mathbf{u_3}$	u <sub>4</sub>	u <sub>5</sub>	u <sub>6</sub>
У1	0	$\frac{-2.1884 e^{-1.4676s} (1 + 28.8135s)}{(1 + 17.522s)(1 + 17.522s)}$	$\frac{-82.032e^{-0.0333s}(l+24.878s)}{(l+8.576s)(l+8.460s)}$	0	$\frac{-2.8  e^{-6.5s}}{1 + 10.98s}$	$\frac{54(l+20.32s)}{(l+18.3s)(l+7.2s)}$
y <sub>2</sub>	61.7	176.2433	0	0	183.3005	0
у <sub>3</sub>	0	176.2433	0	$\frac{96.7}{1+0.1s}$	183.3005	0
y <sub>4</sub>	0	0	541.0021	0	0	0
<b>y</b> 5	0	0	0	$\frac{3.496}{1+0.1s}$	0	0
У <sub>6</sub>	0	176.2433	0	0	0	0

Fig. 8 (b). Transfer function matrix with second-order plus delay approximation for G<sub>16</sub>.

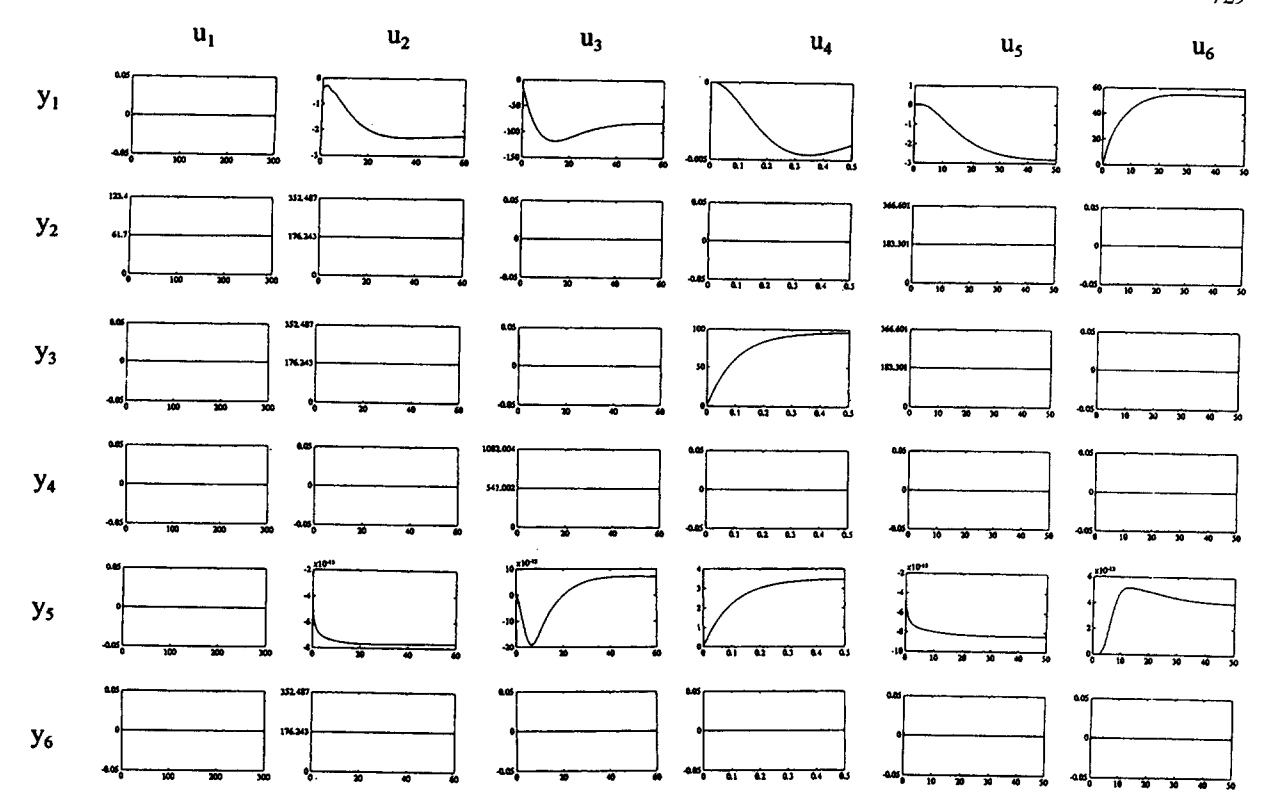


Fig. 9. TBT 95°C-and recycle flow 14420 t/hr.

consequently the existing design methods can only be termed as sub-optimal. In this section, the need to approximate the plant model is removed and a truly optimal design scheme using the unreduced plant model in its nonparametric form is established. Based on this design, a parameter scheduling scheme for adaptive (optimal) control is proposed. The optimality of performance of the control system is maintained over a range of operating conditions against the variation in the linearized plant behaviour due to its nonlinear character. The scheme is illustrated with reference to the top brine temperature (TBT) control of the desalination plant.

This section outlines two aspects:

- a- A nonparametric model-based simulation facility has been developed in the MATLAB framework. This facility has been used in the design of optimal PID controls without involving model reduction or approximation.
- b- A parameter-scheduling scheme for a range of operating conditions has been developed to handle the problem of control of a nonlinear plant by an adaptive control strategy. The method of approach is based on linear designs corresponding to an adequate number of points in the operating region, obtained by extensive simulations and characterizing the resulting controller parameter space as a mapping of the space of plant operating conditions.

 3.1 PID control system simulation and optimization with unreduced plant model in nonparametric form.

Simulation of PID loops with finite-dimensional or parametric models can lead to problems related to dimensionality, numerical conditioning, computational accuracy and stability, etc. This work was in fact motivated by the disappointing experience in the course of simulation attempts in the case of the present model in closed-loop with a PID controller.

The results of MATLAB SIMULINK PID control using this full model (155-dimensional) was quite time-consuming with no consistency. Some were unstable (such as Euler, Runge-Kutta-3 and Runge-Kutta-5).

A nonparametric model such as an impulse response (IR) or step response (SR) model can be obtained either from the original linearized model from MATLAB or more commonly from plant tests. A recursive algorithm, based on discretised convolution using such a model, is proposed here. The burden then is only due to the discretization of these functions. Simple trapezoidal rules of integration would render the algorithm robust to deal with nonparametric models such as IR or SR which pose few problems due to their inherently good behaviour in the case of physical systems. Such an algorithm, that treats the unreduced or unapproximated model as a valuable means by which to design PID control, is given below.

Consider a SISO feedback system with PID controller, as shown in Fig. 10.

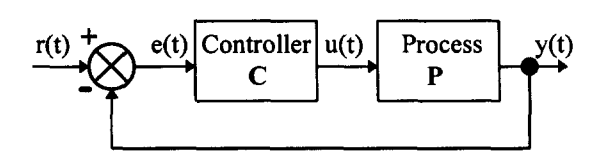


Fig. 10. A SISO feedback control system.

Let the process be described by the sequence  $[p_1, p_2, p_3, p_4, \dots]$  of samples at intervals of  $[O, T, 2T, 3T, \dots]$  of the impulse response function p(t). Define the matrix

$$\mathbf{P} = T \begin{bmatrix} \frac{p_1}{2} & & & & & & \\ \frac{p_2}{2} & \frac{p_1}{2} & & & & & \\ \frac{p_3}{2} & p_2 & \frac{p_1}{2} & & & & \\ \frac{p_4}{2} & p_3 & p_2 & \frac{p_1}{2} & & & & \\ \vdots & \vdots & \vdots & \vdots & \vdots & \vdots & \vdots \\ \frac{p_n}{2} & p_{n-1} & p_{n-2} & p_{n-2} & p_2 & \frac{p_1}{2} \end{bmatrix}$$

and the vectors of samples of the loop signals

$$\mathbf{r} = \begin{bmatrix} r_1 & r_2 & r_3 & r_4 & \dots & r_n \end{bmatrix}^T$$

$$\mathbf{e} = \begin{bmatrix} e_1 & e_2 & e_3 & e_4 & \dots & e_n \end{bmatrix}^T$$

$$\mathbf{u} = \begin{bmatrix} u_1 & u_2 & u_3 & u_4 & \cdots & u_n \end{bmatrix}^T$$

$$\mathbf{y} = \begin{bmatrix} y_1 & y_2 & y_3 & y_4 & \cdots & y_n \end{bmatrix}^T$$

Then,

$$y = Pu$$

$$e = r - y$$

$$u = C y$$

where C is a matrix like P containing the controller information.

#### 3.2 PID Controller.

The output of the controller

$$u(t) = K_c \left[ e(t) + \frac{1}{T_c} \int_0^t e(t) dt + T_a \frac{de}{dt} \right]$$

In terms of the operational matrices (Rao 1983),

$$\mathbf{u} = K_c \left[ \mathbf{l} + \frac{T\mathbf{E}}{T_i} + \frac{Td}{T} \mathbf{D} \right] \mathbf{e} .$$

Therefore, for the PID controller

$$\mathbf{C} = K_C \left[ \mathbf{l} + \frac{T\mathbf{E}}{T_i} + \frac{Td}{T} \mathbf{D} \right].$$

Based on the trapezoidal rule for integration and the backward difference formula for derivative

$$\mathbf{E} = T \begin{bmatrix} 0.5 & & & & & & \\ 0.5 & 0.5 & & & & & \\ 0.5 & 1 & 0.5 & & & & \\ 0.5 & 1 & 1 & 0.5 & & & \\ & & \cdots & \cdots & \cdots & \cdots & \\ 0.5 & 1 & 1 & \cdots & \cdots & 0.5 \end{bmatrix}$$

anc

respectively.

The above give

$$y = [I + PC]^{-1} PC r$$

where I is an identity matrix.

The above algorithm can be written in the following recursive form for implementation in the desired simulation routine:

$$\alpha = \left(1 + \frac{T}{2T_i} + \frac{T_u}{T}\right) ; \quad \beta = \left(1 + \frac{T}{2} P_1 K_c \alpha\right)$$

$$y_1 = \frac{T}{2} P_1 K_c \alpha r_1 / \beta$$

$$e_1 = r_1 - y_1$$

$$u_1 = K_c \alpha e_1$$

$$y_{2} = \frac{\left(\frac{T}{2}P_{2}u_{1} + \frac{T}{2}P_{1}K_{c}\left[\frac{T}{2T_{i}} - \frac{T_{d}}{T}\right]e_{1} + \frac{T}{2}P_{1}K_{c}\alpha r_{2}\right)}{\beta}$$

$$e_{2} = r_{2} - y_{2}$$

$$u_{2} = K_{c} \left[ e_{2} + \frac{T}{2T_{i}} \left( e_{1} + e_{2} \right) + \frac{T_{d}}{T} \left( e_{2} - e_{1} \right) \right]$$

and for k = 3,4, ....

$$y_{k} = \frac{\left\{\frac{T}{2}P_{k}u_{1} + T\sum_{j=2}^{k-1}P_{k-j+1}u_{j} + \frac{T}{2}P_{1}K_{c}\right\}}{\left\{\frac{T}{2T_{i}}e_{1} - \frac{T_{d}}{T}e_{k-1} + \frac{T}{T_{i}}\sum_{k=3}^{n}e_{k-1}\right\} + \frac{T}{2}P_{1}K_{c}\alpha r_{k}}$$

$$e_{k} = r_{k} - u_{k}$$

$$u_{k} = K_{c} \left[ e_{k} + \frac{T}{2T_{i}} \left( e_{1} + e_{k} \right) + \frac{T}{T_{i}} \sum_{k=3}^{n} e_{k-1} + \frac{T_{d}}{T} \left( e_{k} - e_{k-1} \right) \right]$$

If the plant model data is available in the form of a sequence of values of the step response function  $\{s_i, i=1,2,\ldots\}$ , the sequence of impulse response values required for the proposed algorithm can be computed as

$$\left\{ p_{k} = \frac{s_{k+1} - s_{k}}{T}, k = 1,2,... \right\}$$

Alternatively the sequence  $\{p_i\}$  may be replaced with  $\{s_i\}$  and the plant may be driven with the sequence  $\{\Delta u_k\}$  where  $\Delta u_k = \{u_k - u_{k-1}\}/T$ . With either of these modifications, the algorithm can work with the sequence of a step response function. The proposed non-parametric model simulation method is referred to as NONPSIM.

### 3.3 Comparison with other methods with reference to an example.

The results of the present method NONPSIM in the case of the example from (Ogata, 1992) are the best, even better than those due to LINSIM (algorithm in SIMULINK) as is evident from Fig. 11. This experience renders the proposed algorithm most trustworthy.

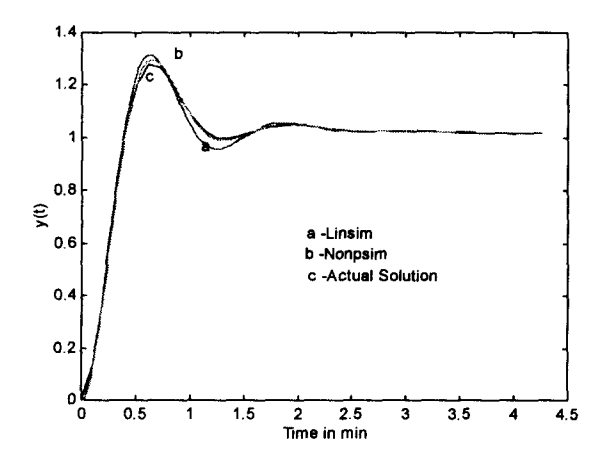


Fig. 11. Step response (a- LINSIM, b- NONPSIM, c- Actual response).

## 3.4 Optimal PID controller design for TBT control in an 18-stage MSF desalination plant by NONPSIM

The IR function was inserted in the present NONPSIM algorithm, and the closed-loop response of the TBT loop with steam controller output was obtained as shown in Fig. 12. Notice that the response obtained through LINSIM routine from SIMULINK is considerably time consuming and slightly different from the results of NONPSIM. In view of the experience gained with the simple textbook example, it is assumed that the present method is reliable, as the discretization interval has been reduced to the limit below which the results are not significantly improved further.

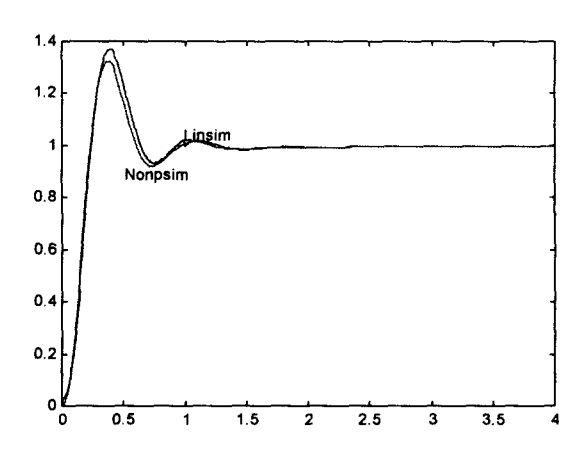


Fig. 12. Unit step response of the TBT control loop in an MSF Plant.

Use of an integral performance criterion often results in a better closed-loop response of a control system than heuristic tuning methods, since the method takes into account the whole transient response of the system.

The results of optimization with reference to the four well known (Zhuang and Atherton, 1991) integral performance criteria, viz., ISE, IAE, ISTE and ITAE are obtained by simulation using the nonparametric model of the plant at a particular operating point. Together with the presently created simulation facility, the FMINS optimization routine from MATLAB toolbox has been invoked. FMINS searches for optimal PID controller parameters.

Several approaches to improve PID tuning above the level of quality achieved by Ziegler-Nichols' (Z-N) method, have been reported in the literature (Ziegler and Nichols, 1942). In (Astrom and Hagglund, 1984) a tuning method based on phase margin was reported. In (Astrom et al., 1993) a refinement of the Z-N method was suggested. In the works of (Zhuang and Atherton, 1991) the tuning methods are based on optimization in the time domain. The Ziegler-Nichols' or those corresponding to the FODT form can be used to initiate the algorithm.

Table (3) gives the optimal PID controller parameters for plant operation at the chosen point (TBT 95°C Recy. flow 14420 t/hr). Figure 13 gives the corresponding unit step response function of the optimally controlled closed-loop system.

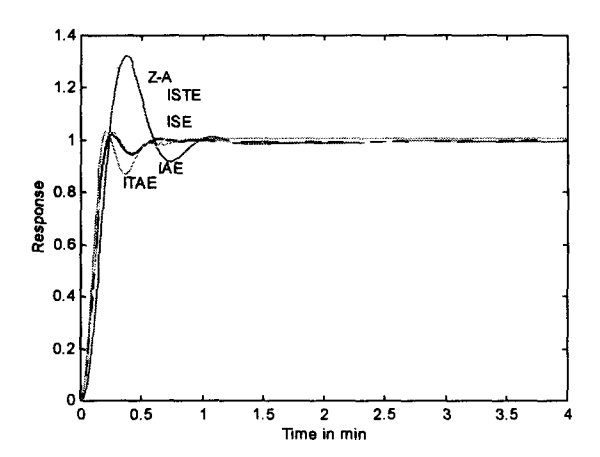


Fig. 13. Step response with optimal control settings.

### 3.5 Parameter-scheduling scheme for a range of operating conditions

It is clear that a fixed PID controller cannot be optimal if the operating point changes from the one at which the optimal controller was designed in the presence of nonlinear behaviour. In this section the parameter variations in the linearised plant model have been modelled over the operating region of interest, and these are mapped into the parameter space of the optimal PID controller.

#### 3.6 The space of operating conditions of the plant.

Based on the studies and plant operating experience, the most important of the plant operating conditions to be enlisted in the space are:

T = Top brine temperature (TBT)

F = Brine recycle flowrate

These two are fixed according to the requirements of the plant production rate, simultaneously satisfying other important conditions such as performance ratio. There are limits set on these variables for practical reasons. For example, an upper limit on T is set in view of the plant's vulnerability to scaling, and a lower limit on the velocity of brine through the tubes (thereby on F) to avoid sludge formation. Likewise, a lower limit on T and a higher limit on the velocity of brine in the tubes (thereby on F) are based on certain other conditions. If the ranges of TBT and brine recycle flow are denoted by  $[T_{\min}, T_{\max}]$  and  $[F_{\min}, F_{\max}]$ respectively, and a set of operating conditions  $\{T_k, F_k, k = 1, 2, ..., N\}$  is considered in this region, the optimal PID controller parameter vector  $\mathbf{c}_k = [K_{pk}T_{lk}T_{ak}]$  for k = 1, 2, ..., N is obtained by the simulation facility developed earlier.

3.7 Mapping of the plant operating condition space into controller parameter space.

The two-dimensional space of plant operation conditions is sampled as

$$\{T_k ; F_k, k=1,2,...,N\}$$
.

At each of these points, the controller parameter vectors are given by

$$\mathbf{c}_{k} = \begin{bmatrix} K_{pk} & T_{ik} & T_{dk} \end{bmatrix}$$
.

In view of the not too wide variations in T and F, a mapping function of the form

$$c = f(T, F)$$

is considered, or

$$c_1 = f_1(T, F) = a_{11} + a_{12}T + a_{13}F + a_{14}TF = K_p$$

$$c_2 = f_2(T, F) = a_{21} + a_{22}T + a_{23}F + a_{24}TF = T_i$$

$$c_3 = f_3(T, F) = a_{31} + a_{32}T + a_{33}F + a_{34}TF = T_d$$

Using the relations established at the points 1,2,...,N, the coefficients in the vector function **f** are determined by least-squares fitting to form the parameter-scheduling law for a chosen optimization criterion.

A convenient form of this adaptive law is

$$\mathbf{c} = \begin{bmatrix} a_{11} & a_{12} & a_{13} & a_{14} \\ a_{21} & a_{22} & a_{23} & a_{24} \\ a_{31} & a_{32} & a_{33} & a_{34} \end{bmatrix} \begin{bmatrix} 1 \\ T \\ F \\ TF \end{bmatrix} = \begin{bmatrix} K_p \\ T_i \\ T_d \end{bmatrix}.$$

#### 3.8 Parameter-scheduling law for the plant.

Table 3 gives the PID controller parameters obtained by simulation on the unreduced plant. The Zhuang-Atherton results which are based on FODT approximation of the plant are given in the last rows of this table. The parameter-scheduling strategies obtained by least-squares fitting of the results in the case of the four optimizing criteria are given by the following:

ISE:

$$\mathbf{c} = \begin{bmatrix} 0 & -0.0076 & -0.0174 & 0.0002 \\ 0 & 0.0086 & 0.0392 & -0.0003 \\ 0 & 0.0076 & 0.0028 & -0.00005 \end{bmatrix} \begin{bmatrix} 1 \\ T \\ F \\ TF \end{bmatrix}$$

IAE:

$$\mathbf{c} = \begin{bmatrix} 0 & -0.0067 & -0.0141 & 0.0002 \\ 0 & 0.0165 & 0.1102 & -0.0010 \\ 0 & 0.0061 & 0.00299 & -0.00005 \end{bmatrix} \begin{bmatrix} 1 \\ T \\ F \\ TF \end{bmatrix}$$

ITAE:

$$\mathbf{c} = \begin{bmatrix} 0 & -0.0164 & -0.0486 & 0.0006 \\ 0 & -0.0290 & 0.1549 & -0.0013 \\ 0 & 0.0032 & 0.0045 & -0.0001 \end{bmatrix} \begin{bmatrix} 1 \\ T \\ F \end{bmatrix}$$

ISTE:

$$\mathbf{c} = \begin{bmatrix} 0 & -0.0035 & 0.0083 & -0.00002 \\ 0 & 0.02262 & 0.1608 & -0.00151 \\ 0 & 0.0044 & -0.00224 & 0.00001 \end{bmatrix} \begin{vmatrix} 1 \\ T \\ F \\ TF \end{vmatrix}$$

**Table 3 Optimal PID Controller Parameters** 

Case	TRT	Rec.	Crite-	Par	ameters o	f PID
Casc	101	Flow	rion	Controllers		
	°C	t/hr	11011	$\overline{K_p}$	Ti	$T_d$
1	95	14420	ISE	0.7346	2.6647	0.2734
1	93	14420	IAE	0.8007	5.3364	0.1814
			ITAE	0.8246	4.7709	0.1781
			ISTE	1.4234	6.5527	0.0809
			Z-A	1.1244	7.3047	0.0409
	100	14420	ISE	0.8120	2.5166	0.2521
_			IAE	0.9087	3.9736	0.1541
			ITAE	1.5880	4.1986	0.0670
			ISTE	0.8654	4.2280	0.1727
			Z-A	1.2113	5.5913	0.0432
3	105	14420	ISE	1.2292	2.05	0.2219
			IAE	1.2162	3.0922	0.1226
			ITAE	2.1436	0.2816	0.0715
			ISTE	1.2893	3.0901	0.1506
			Z-A	1.8782	5.2330	0.0371
4	105	11500	ISE	0.8108	1.8366	0.3492
			IAE	0.8271	2.8149	0.2307
			ITAE	1.4653	0.5759	0.1142
			ISTE	0.8678	2.8599	0.2304
			Z-A	1.1870	4.9570	0.0485
5	105	12500	ISE	0.8547	1.8909	0.2921
			IAE	0.9050	2.7296	0.1918
			ITAE	1.5071	0.5320	0.0929
			ISTE	0.9002	2.7488	0.2038
			Z-A	1.3930	4.7228	0.0439
6	105	13500		1.1174	1.8207	0.2874
			IAE	1.1301	3.0086	0.1632
			ITAE	2.0084	3.3760	0.0917
			ISTE	1.1906	3.0579	0.1844
			Z-A	1.4993	4.2107	0.0413

The PID controllers obtained here are truly optimal. The tuning algorithm has been tried in several different cases of plant models and has produced good results.

#### 4. CONCLUSIONS

The work presented in this paper is the culmination of systematic efforts at advancing the present state of control methodology in the desalination industry. Figure 14 above shows the overall integrated scheme that is realized here. The parameter scheduling law derived here for a plant actually operating in Abu Dhabi in the United Arab Emirates (where the

world's largest MSF unit is expected to be commissioned in 1996) is a step forward in the application of advanced control.

The control strategy proposed here is designed to handle the nonlinear character of the plant. The present parameter-scheduling law is expected to be of use in conjunction with a steady-state optimization program at a higher level of hierarchy to provide optimal operating conditions as setpoint values for T and F. These will automatically schedule the controller parameters according to the law presented here, to ensure dynamic optimization according to the chosen integral performance criterion.

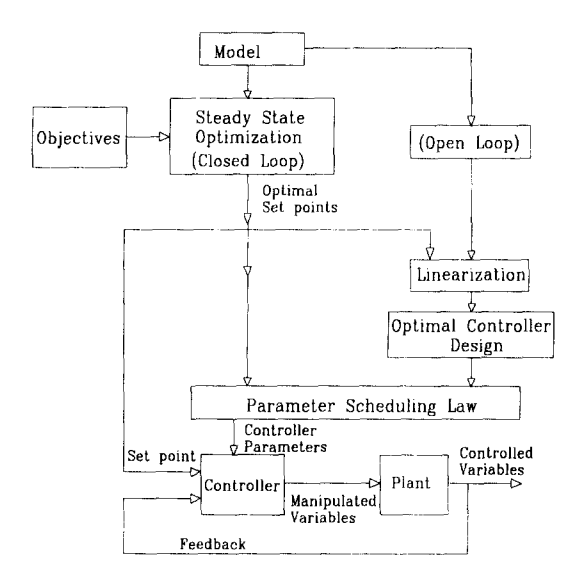


Fig. 14. The integrated adaptive control scheme.

#### **REFERENCES**

Al-Gobaisi, D.M.K., A.S. Barakzai and A.M. El-Nashar (1991). An overview of modern control strategies for optimizing thermal desalination plants, in M. Balaban (Ed.) Proceedings of the 12th International Symposium on Desalination and Water Reuse, Malta.

Al-Gobaisi, D.M.K., A. Hassan, G.P. Rao, A. Sattar, A. Woldai and R. Borsani (1993). Towards improved automation for desalination process, Part-I: Advanced Control, *Proceedings of the IDA/WRPC World Conferences on Desalination and Water Treatment*, Yokohama, Japan.

Al-Gobaisi, D.M.K. (1995). Conceptual specification for improved automation and total process care in large scale desalination plants of the future, *Desalination*, 95, pp. 287-297, Elsevier Science B.V., Amsterdam.

Astrom K.J., T. Hagglund C.C. Hang and W.K. Ho (1993). Automatic tuning and adaptation for PID controllers - Survey. *Control Eng. Practice* Vol. 1 No. 4 pp. 699-714.

Astrom, K.J. and T. Hagglund (1984). Automatic tuning of simple regulators with specifications

on phase and amplitude margins, *Automatica*, **20** pp 645-651.

- Barba, D., G. Linzzo and G. Tagliferri (1973). Mathematical model for multiflash desalting plant control. 4th Int. Symp. on Fresh Water from Sea Vol. 1, 153-168.
- Husain, A., A. Woldai and A. Al-Radif (1993).

  Modelling and simulation of multistage flash (MSF) desalination plant; paper presented at IDA/WRPC Conference on Desalination and Water Reuse, Yokohama, Japan.
- Ogata, K. (1992). Modern Control Engineering, 2nd edition, Prentice Hall, pp 602-603.
- Rao, G.P. (1983). Piecewise constant orthogonal functions and their application to systems and control. Lecture notes in Control and Information Sciences, Springer-Verlag.

- Seborg, D.E., T.F. Edgal and D.A. Mellichanp (1989). Process dynamics and control, John Willey, NY.
- Smith, A.C. and A.B. Corripio (1985). Principles and practice of automatic process control, John Willey and Sons.
- Unbehauen, H. and G.P. Rao (1987). Identification of Continuous Systems, North Holland.
- Zhuang M. and D.P. Atherton (1991). Tuning PID controllers with integral performance criteria, *Proceedings of IEE conference on Control*, No. 332, Vol. 1, pp 481-486.
- Zhuang M. and D.P. Atherton (1993). Automatic tuning of optimum PID controllers, *IEE Proceedings-D*, Vol. 140, No. 3.
- Ziegler, J.G. and N.B. Nichols (1942). Optimum settings for automatic controllers, *Trans. ASME*, **64**, pp. 759-768.